Noise analysis in a seeded four-wave mixing process generated in a photonic crystal fiber pumped by a chirped pulse

Theo Guilberteau, Coralie Fourcade-Dutin, Frederic Fauquet, Romain Dauliat, Raphael Jamier, Hector Muñoz-Marco, Pere Perez-Millan, Philippe Roy, Patrick Mounaix, Damien Bigourd

Noise analysis in a seeded-Four Wave Mixing process generated in a photonic crystal fiber pumped by a chirped pulse.

THEO GUILBERTEAU,[1] CORALIE FOURCADE-DUTIN,[1] FREDERIC FAUQUET,[1] ROMAIN DAULIAT,[2] RAPHAEL JAMIER,[2] HECTOR MUÑOZ-MARCO,[3] PERE PEREZ-MILLAN,[3] PHILIPPE ROY,[2] PATRICK MOUNAIX,[1] DAMIEN BIGOURD[1*]

[1]*Laboratoire IMS, UMR CNRS 5218, University of Bordeaux, 33400 Talence, France*
[2]*Université Limoges, XLIM, UMR CNRS 7252, F-87000 Limoges, France*
[3]FYLA LASER SL, Ronda Guglielmo Marconi 12, 46980, Paterna (Valencia), Spain
**Corresponding author: damien.bigourd@u-bordeaux.fr*

Received XX Month XXXX; revised XX Month, XXXX; accepted XX Month XXXX; posted XX Month XXXX (Doc. ID XXXXX); published XX Month XXXX

Four wave mixing is investigated when chirped pump and signal pulses are injected in a photonic crystal fiber. The shot-to-shot stability of the amplified coherent signal was measured by using the dispersive Fourier transform method and compared with numerical simulations. We highlighted the SNR of the pulsed signal increases with the injected power and showed that it is not deteriorated through the amplification when the fiber optical parametric amplifier is strongly saturated. The SNR of the signal remains nearly constant after the amplifier.

Four-wave mixing (FWM) has been extensively investigated in optical fibers since it provides a high-gain value and a large gain-bandwidth with an adjustable central wavelength [1-4]. For these reasons, FWM based parametric amplifier is currently a promising technology to deliver ultra-short pulses when a photonic crystal fiber (PCF) is injected by pump and signal pulses [5-9]. However, as any phase insensitive optical amplifier, FWM is also subject to amplified spontaneous emission, often called parametric fluorescence i.e., parametric amplification of the quantum noise due to a two-photon emission from two pump photons. In the case of FWM based amplification of ultra-short pulse, a chirped pump pulse is injected in a designed PCF together with a signal chirped pulse. At the output, the signal is compressed near the Fourier transform limit [1,5-9]. The instantaneous frequencies of the broadband fluorescence are generated with temporal and spectral distributions according to the phase-matched FWM relation and the pump chirp [2,10] while the amplified signal has a distribution that mostly follows its initial chirp. At the amplifier output, the signal is selected but the spontaneous emission of the incoherent parametric fluorescence degrades the amplification quality and the shot-to-shot stability.

Some works have already been achieved in bulk crystals to extract the contribution of fluorescence from the parametric amplification of ultra-short pulse [11,12]. FWM based parametric amplification has also been investigated for its noiseless amplification feature to potentially develop ultra-low noise amplifier in the continuous wave regime [13]. In the ideal case, the amplification can reach a 3-dB quantum-limited noise figure in a phase insensitive amplifier although few other noise sources, as the Raman effect [14] or pump transferred noise [15], add their non-negligible contributions. In addition, it has been shown that the noise properties of modulation instability driven the supercontinuum generation, in the anomalous regime, depends strongly on the presence of a weak seed which provides a deterministic growth limiting the contribution of the broadband noise [16-17]. However, the output stability is directly linked to the fluctuation of the input signal. In our case, as we focused on FWM based amplification of a signal, the peak power is limited such as a continuum is not generated. In this work, we investigate the noise and signal stability after FWM based amplification by measuring the gain value and the signal to noise ratio by recording an ensemble of single shot FWM spectra thanks to the dispersive Fourier transform Method [18,19].

The experimental set-up, shown in Figure 1, was developed to highlight the chirped signal amplification through the fiber optical parametric amplifier and to investigate its stability. The pump pulse is generated from a mode-locked oscillator (Flint, Light Conversion) delivering a train of pulses at 76 MHz with a duration of 80 fs (at full

width at half maximum-FWHM) and a spectrum centered at 1030 nm. A part of the oscillator output is injected in a volume Bragg grating (VBG) that stretches the pulses to a duration of ~50 ps and an acousto-optic modulator to decrease the repetition rate to 1 MHz. Then the pulses seed several ytterbium doped fiber amplifiers to increase the average power to a maximum of 1 W. The spectral bandwidth is measured at 6 nm (FWHM). The pump pulse is then injected in a 5-meter-long PCF with a zero-dispersion wavelength at 1028 nm [20]. It means the pump spectrum lies mostly in the anomalous dispersion regime. Two FWM lobes are observed with an optical spectrum analyzer (OSA) and they are located around 1000 and 1077 nm for a peak power of 300 W (Figure 2.a, red curve). Another part of the oscillator is used to generate a continuum in a 7 cm long all normal dispersion (ANDI) fiber extending from 960 to 1100 nm [21]. The spectral broadening mechanism is mainly due to self-phase modulation and optical wave-breaking ensuring a low noise level and high degree of coherence when the fiber is pumped in the fs regime [22,23].

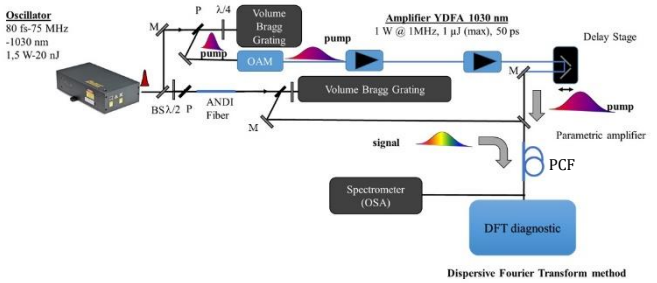

Fig. 1. Experimental set-up. AOM, acousto-optic modulator; YDFA, Ytterbium Doped Fiber Amplifier; PCF, photonic crystal fiber; OSA, Optical Spectrum Analyzer; ANDI fiber, all normal dispersion fiber.

A second chirped VBG selects a spectrum part of the continuum (Figure 2 black curve) centered at 1077 nm with a bandwidth of 13 nm at full width at half maximum (FWHM). The pulse duration is ~150 ps corresponding to a chirp rate of 11.5 ps/nm. When this chirped signal pulse is injected in the PCF with an average power of 20 µW together with the chirped pump pulse, the signal is amplified (Figure 2, blue curve) with a gain of 35 dB. In this case, the relative delay between the signal and pump pulses has been tuned to get the maximum gain. At the PCF output, single shot spectra are recorded by a dispersive Fourier transform (DFT) set-up with a 4.6 km long fiber (SMF28), a fast photodiode and an oscilloscope with a maximum bandwidth of 8 GHz [18,19]. Once the PCF output is injected in the DFT measurement device, the pulse spectrum is temporally dispersed resulting in a time to frequency mapping. The temporal waveform recorded with the fast photodiode allows real time measurement of single-shot spectral fluctuations. As an example, Figure 3.a shows a superposition of 500 single shot spectra (blue curves) and the averaged curve (red curve) recorded with the DFT method. To accurately reconstruct the DFT time-frequency mapping, we used both second and third order dispersion coefficients of the SMF (β_2=17 ps^2/km, β_3=-0.0134 ps^3/km) and a general good agreement has been obtained with the spectrum recorded by the OSA (Fig. 2). However, the signal bandwidth recorded with the DFT set-up is narrower (~7 nm) and depends on the injection of the PCF output in the SMF.

From the ensemble of single shot spectra, the signal to noise ratio (SNR) is measured from the ratio between the average value and its standard deviation (Figure 3.b). The SNR at the pump wavelength is higher than 20 and is spectrally modulated due to the saturation of the FWM process; i.e the pump depletion. The maximum SNR at the signal wavelength is ~22 after amplification in the FWM process while we measured it at ~23 when the pump was not launched in the PCF (i.e without any amplification). Thus, the amplification does not significantly degrade the shot-to-shot stability of the signal pulse even at high gain. From this SNR comparison, we can also conclude that the SNR is mostly linked to the signal stability rather that the fluorescence emission or the pump fluctuation. We also measured the gain and SNR as the function of the injected signal power to understand the origin of the SNR stable value (Figure 4). The two plots have been recorded successively and the measurement have been done several times to confirm the general behavior. The parametric amplifier strongly saturates since the gain decreases from ~43 dB to 35 dB when the signal power increases. This saturation is an important advantage since it provides stability of the amplified signal such that, the signal output power increases when the input decreases acting as a negative feedback [24,11]. This intensity fluctuation limitation allows to get a relatively high SNR value, similar to the input one. It is important to note that the pump power is not significantly depleted. Some back conversion from the signal to the pump may arise for stronger input power [1].

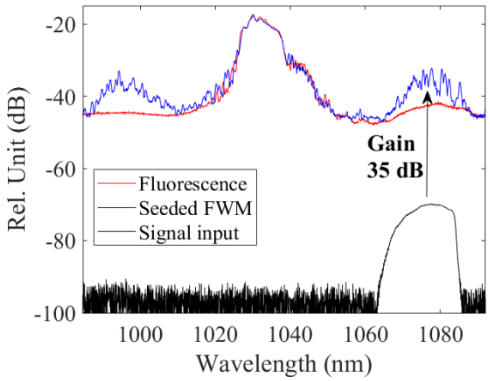

Fig. 2. Spectrum recorded with an OSA. The fluorescence (red line) and seeded FWM (blue line) spectra have been obtained for a pump power of 300 W. The seed spectrum is displayed with black lines.

In order to deeply understand the role of the amplification in the signal stability, we performed numerical simulations by integrating the nonlinear Schrödinger equation with the split-step method including the fiber dispersion and nonlinearity as the Kerr effect and Raman response. As for the experimental parameter, the input pump pulse has a chirp of ~8.3 ps/nm with a spectral bandwidth of 6 nm (FWHM) centered at 1030 nm leading to a pulse duration of 50 ps (FWHM). In comparison with the experiment, we intentionally decrease the pulse duration to limit the computational time. The pulse is injected in a lossless photonic crystal fiber (PCF) which has a nonlinear coefficient of 11 W^{-1}.km^{-1} and a length of 5 m. The zero-dispersion wavelength (ZDW) is at 1028 nm. A quantum noise δ_q is added to the total electric field at the PCF input. This pulse shot noise is described semi-classically by adding a noise seed of one photon per mode with random phase on each spectral discretization bin [25]. 1000 simulations have been performed with different input noise conditions. Figure 5.a shows the ensemble of spectra (black line) and the average (red line) for an input peak

power 150 W. Two FWM lobes are clearly observed at around 990 and 1074 nm.

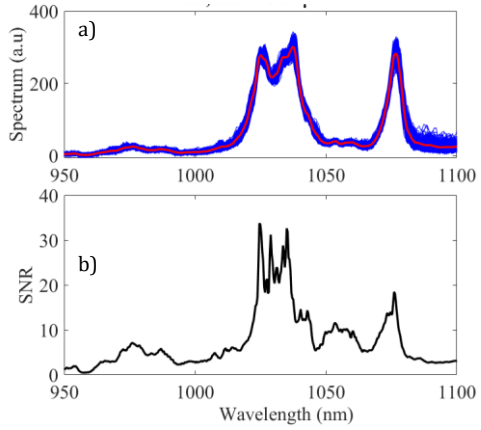

Fig. 3. a) FWM bands detected with the DFT set-up. The averaged spectrum (red line) of 500 single shots (blue lines) are displayed. b) SNR as the function of the wavelength.

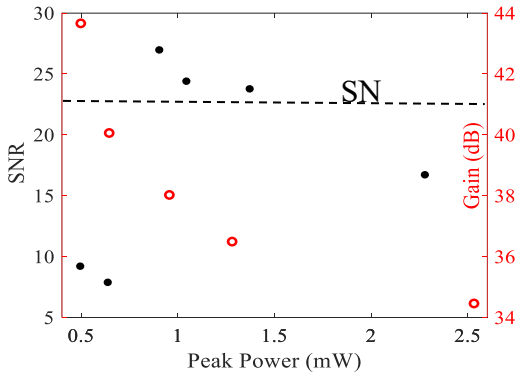

Fig. 4. SNR and gain as the function of the peak power of the signal

Then the signal has been injected in the PCF together with the pump pulse. The input signal spectrum has a bandwidth of 13 nm (FWHM) and the chirp is 11.5 ps/nm. These values are chosen to fit with the experimental parameters. The peak power P_{sig} is 1 mW. When the signal is simultaneously injected with the chirped pump pulse, the signal is amplified and the spectrum becomes narrower with a bandwidth of 1.2 nm. This gain narrowing depends on the signal chirp relative to the fluorescence spectrogram. In fact, the PCF dispersion and pump properties define the time-frequency distribution of the parametric amplification. The chirp signal should agree with the time-frequency distribution for a maximum amplification [1]. The larger gain bandwidth obtained during the experiment is attributed to the inhomogeneity of the PCF dispersion profile since it can modify the time-frequency distribution of the amplification [26,27].

In the following, we also added a second noise source to consider the seed amplitude fluctuation δ. When the continuum is generated from an ANDI fiber, the amplitude fluctuation of the laser contributes mostly to the noise whereas δ_q is insignificant [23]. Several works have shown that the relative intensity noise of the continuum is at similar level of the laser source [23,28-29]. Therefore, we only consider the seed amplitude fluctuation and neglect jitter shot to shot variation for our long-chirped pulse. In our work, we added the term $\delta\sqrt{P_{sig}}$ to the signal electric field with δ being an adjustable random value with a Normal distribution and P_{sig} the signal power. For various δ value, the SNR has been calculated and Figure 6 shows an example of the SNR as the function of the wavelength for a peak power of the signal equals to 0.5 mW or 150 mW. The pump SNR significantly decreases at the spectrum center due to the saturation effect. This curve has a similar behavior than the spectrum (Figure 5) exhibiting a strong depletion with the signal amplification. The signal SNR has a high value and is narrow as expected from its spectrum. At high seed power, the SNR of the signal increases significantly confirming that the saturation of the amplifier leads to a better SNR value.

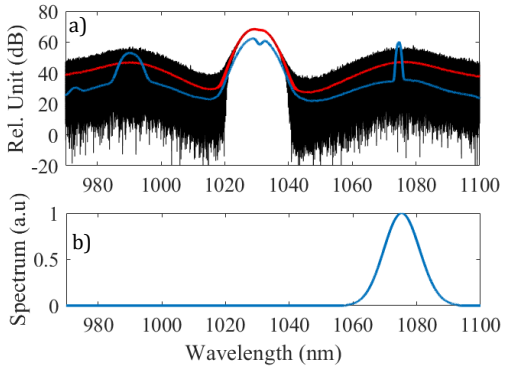

Fig. 5. a) 1000 single shot simulated spectra (black lines) and their average (red line). The average spectrum of the seeded FWM is displayed in blue b) Normalized seed spectrum

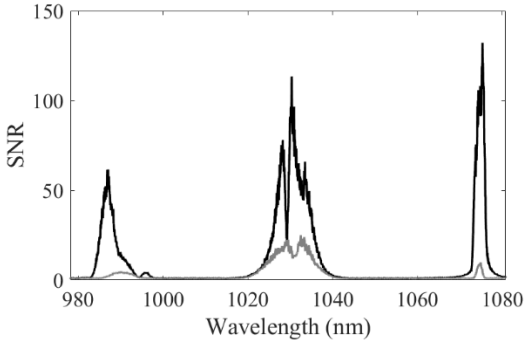

Fig. 6. SNR as the function of the wavelength for δ=0.01 and a signal peak power of 0.5 mW (grey curve) and 150 mW (black curve).

The gain has also been calculated as the function of the peak power of the injected signal (black dashed line in Figure 7). As in the experiment, it decreases from 40 dB to 18 dB when the power increases confirming the strong saturation of the parametric amplifier. The SNR has also been analyzed from the ensemble of single shot spectrum for each case. When δ=0, it increases with the signal power since the number of determinist photons is higher while the fluorescence does not increase.

When the fluctuation coefficient δ=0.01 (red curve in Figure 7.a),

the SNR is mostly affected by the fluorescence at low signal power. It increases and reaches a constant value at ~0.05 W. At high signal power, the SNR is slightly higher than the injected SNR (equals to 125) due to the strong saturation of the amplifier and the weak contribution of the fluorescence. When the fluorescence contribution is removed in the simulation (grey symbols in Figure 7.a), the SNR increases and is higher that the injected one even at low power. In order to see the influence of the fluctuation input on the SNR, we reproduce the simulation for various δ values (Figure 7.b). Of course, the input SNR decreases when δ increases (dashed horizontal lines). The evolution of the SNR is similar in all cases and it reaches a constant value higher than the input one.

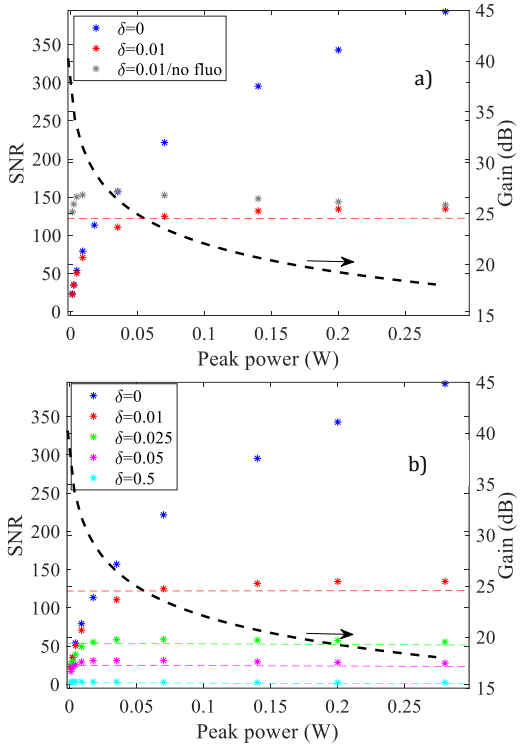

Fig. 7. a) SNR and gain as the function of the peak power of the signal for δ=0.01 or 0 with or without the fluorescence. b) SNR and gain as the function of the peak power for various δ value. The horizontal dashed lines represent the SNR value at the input.

In conclusion, the shot-to-shot stability of seeded FWM has been investigated when chirped pump and signal pulses are injected in a photonic crystal fiber. By using the DFT method, we highlighted that the SNR value of the amplified signal can be similar to the injected one due to the saturation regime providing a negative feedback. This effect has been observed in numerical simulations and confirms that the SNR of the amplified signal can be similar to the input one. This information is very important since it proves that the fiber optical parametric amplifier does not provide any additional fluctuations when it is strongly saturated if the noise floor is not given by the parametric fluorescence.

Funding This work was supported by the IdEx University of Bordeaux / Grand Research Program LIGHT.

Data availability. Data underlying the results presented in this paper are not publicly available at this time but may be obtained from the authors upon reasonable request.

Disclosures. The authors declare no conflicts of interest.

References

1. C Fourcade-Dutin, O Vanvincq, A Mussot, E Hugonnot and D Bigourd, J. Opt. Soc. Am B **32**, 1488 (2015).
2. O Vanvincq, C Fourcade-Dutin, A Mussot, E Hugonnot and D Bigourd, J. Opt. Soc. Am B **32**, 1479 (2015).
3. Y. Zhou, K. K. Y. Cheung, S. Yang, P. C. Chui and K. K. Y. Wong, Opt. Lett. **34**, 989 (2009).
4. R. Becheker, M. Touil, S. Idlahcen, M. Tang, A. Haboucha, B. Barviau, F. Grisch, P. Camy, T. Godin and A. Hideur, Opt. Lett. **45**, 6398 (2020).
5. D. Bigourd, L. Lago, A. Mussot, A. Kudlinski, J.F. Gleyze and E. Hugonnot, Opt. Lett. **35**, 3840 (2010).
6. Y. Qin, O. Batjargal, B. Cromey and K. Kieu, Optics Letters **28**, 2317 (2020).
7. Y. Qin, Y.H Ou, B. Cromey, O. Batjargal, J. K. Barton and K. Kieu, Opt. Lett. 44, 3422 (2019).
8. M. L. Buttolph, P. Sidorenko, C. B. Schaffer, F. Wise, Optics Letters, **47**, 545 (2022).
9. L. Lafargue, F. Scol, O. Vanvincq, E. Poeydebat, G. Bouwmans E. Hugonnot, Optics Letters **47**, 4347 (2022).
10. D. Bigourd, P. Beaure d'Augeres, J. Dubertrand, E. Hugonnot and A. Mussot, Opt. Lett. **39**, 3782 (2014).
11. C. Manzoni, J. Moses, F. X. Kärtner and G. Cerullo, Opt. Express **19**, 8357 (2011).
12. N.H. Stuart, D. Bigourd, R.W. Hill, T.S. Robinson, K. Mecseki, S. Patankar, G.H.C. New and R.A. Smith, Opt. Comm. **336**, 319 (2015).
13. Z. Tong, A. Bogris, M. Karlsson and P. A. Andrekson, Opt. Express **18**, 2884 (2010).
14. P. L. Voss and P. Kumar, Opt. Lett. **29**, 445 (2004).
15. A. Durecu-Legrand, C. Simonneau, D. Bayart, A. Mussot, T. Sylvestre, E. Lantz and H. Maillotte, IEEE Photon. Technol. Lett. 17, 1178 (2005).
16. S. T. Sørensen, C. Larsen,U. Møller, P. M. Moselund, C. L. Thomsen and Ole Bang, J. Opt. Soc. Am. B **29**, 2875 (2012).
17. D. R. Solli, C. Ropers, and B. Jalali, Phys. Rev. Lett. **101**, 233902 (2008).
18. T. Godin et al. Advances in Physics : X **7**, 2067487 (2022).
19. P. Robert, C. Fourcade-Dutin, R. Dauliat, R. Jamier, H. Muñoz-Marco, P. Pérez-Millán, H. Maillotte, J. Dudley, P. Roy, D. Bigourd, Optics Letters 45, 4148 (2020).
20. C. Fourcade-Dutin, A. Imperio, R. Dauliat, R. Jamier, H. Muñoz-Marco, P. Pérez-Millán, H. Maillotte, P. Roy and D. Bigourd, Photonics **6**, 20 (2019).
21. C. Fourcade-Dutin and D. Bigourd, Appl. Phys. B 124, 154 (2018).
22. E. Genier, P. Bowen, T. Sylvestre, J. M. Dudley, P. Moselund and O. Bang, J. Opt. Soc. Am. B **36**, A61 (2019).
23. A. M. Heidt, J. S. Feehan, J. H. V. Price and T. Feurer, J. Opt. Soc. Am. B **34**, 764 (2017).
24. K. Inoue and T. Mukai, J. Lightwave Technol. 20, 969(2002).
25. J. M. Dudley, G. Genty and S. Coen, Rev. Mod. Phys. **78**, 1135 (2006).
26. C. Fourcade-Dutin, F. Fauquet, P. Mounaix, D. Bigourd, *IEEE Phot. Technol. Lett. Submitted.*
27. C. Fourcade-Dutin and D. Bigourd, J. Mod. Opt. **64**, 500 (2017).
28. N. Nishizawa and J. Takayanagi, J. Opt. Soc. Am. B **24**, 1786 (2007).
29. Y. Liu, Y. Zhao, J. Lyngso, S. You, W.L. Wilson, H. Tu and S.A. Boppart, J. Lightwave Technol. **33**, 1814 (2015).

References with title

1. C Fourcade-Dutin, O Vanvincq, A Mussot, E Hugonnot and D Bigourd, "Ultra-broad band fiber optical parametric amplifier pumped by chirped pulses Part II: Sub-30 fs pulse amplification at high gain," J. Opt. Soc. Am B **32**, 1488 (2015).
2. O Vanvincq, C Fourcade-Dutin, A Mussot, E Hugonnot and D Bigourd, "Ultrabroadband fiber optical parametric amplifiers pumped by chirped pulses. Part 1: analytical model" J. Opt. Soc. Am B **32**, 1479 (2015).
3. Y. Zhou, K. K. Y. Cheung, S. Yang, P. C. Chui and K. K. Y. Wong, "Widely tunable picosecond optical parametric oscillator using highly nonlinear fiber," Opt. Lett. 34, 989 (2009).
4.Rezki Becheker, Mohamed Touil, Saïd Idlahcen, Mincheng Tang, Adil Haboucha, Benoit Barviau, Frédéric Grisch, Patrice Camy, Thomas Godin, and Ammar Hideur, "High-energy normal-dispersion fiber optical parametric chirped-pulse oscillator," Opt. Lett. 45, 6398 (2020).
5. D. Bigourd, L. Lago, A. Mussot, A. Kudlinski, J.F. Gleyze and E. Hugonnot, "High-gain, optical-parametric, chirped-pulse amplification of femtosecond pulses at 1 µm," Opt. Lett. **35**, 3840 (2010).
6. Y. Qin, O. Batjargal, B. Cromey, K. Kieu, "All-fiber high-power 1700 nm femtosecond laser based on optical parametric chirped pulse amplification," Optics Letters **28**, 2317 (2020).
7. Y. Qin, Y.H Ou, B. Cromey, O. Batjargal, J. K. Barton and K. Kieu, "Watt-level all-fiber optical parametric chirped-pulse amplifier working at 1300 nm"Opt. Lett. 44, 3422 (2019).
8. M. L. Buttolph, P. Sidorenko, C. B. Schaffer, F. Wise, "Femtosecond optical parametric chirped pulse amplification in birefringent step-index fiber," Optics Letters, **47**, 545 (2022).
9. L. Lafargue, F. Scol, O. Vanvincq, E. Poeydebat, G. Bouwmans E. Hugonnot, "All-polarization-maintaining and high energy fiber optical parametric chirped-pulse amplification system using a solid core photonic hybrid fiber," Optics Letters **47**, 4347 (2022).
10. D. Bigourd, P. Beaure d'Augeres, J. Dubertrand, E. Hugonnot and A. Mussot, "Ultra-broadband fiber optical parametric amplifier pumped by chirped pulses," Opt. Lett. **39**, 3782 (2014).
11. C. Manzoni, J. Moses, F. X. Kärtner and G. Cerullo, "Excess quantum noise in optical parametric chirped-pulse amplification," Opt. Express **19**, 8357 (2011).
12. N.H. Stuart, D. Bigourd, R.W. Hill, T.S. Robinson, K. Mecseki, S. Patankar, G.H.C. New and R.A. Smith, "Direct fluorescence characterisation of a picosecond seeded optical parametric amplifier," Opt. Comm. **336**, 319 (2015).
13. Z. Tong, A. Bogris, M. Karlsson and P. A. Andrekson, "Full characterization of the signal and idler noise figure spectra in single-pumped fiber optical parametric amplifiers," Opt. Express **18**, 2884 (2010).
14. P. L. Voss and P. Kumar, "Raman-noise-induced noise-figure limit for χ(3) parametric amplifiers," Opt. Lett. **29**, 445 (2004).
15. A. Durecu-Legrand, C. Simonneau, D. Bayart, A. Mussot, T. Sylvestre, E. Lantz and H. Maillotte, "Impact of pump OSNR on noise figure for fiber-optical parametric amplifiers," IEEE Photon. Technol. Lett. 17, 1178 (2005).
16. S. T. Sørensen, C. Larsen,U. Møller, P. M. Moselund, C. L. Thomsen and Ole Bang1,2, "Influence of pump power and modulation instability gain spectrum on seeded supercontinuum and rogue wave generation," J. Opt. Soc. Am. B **29**, 2875 (2012).
17. D. R. Solli, C. Ropers, and B. Jalali, "Active Control of Rogue Waves for Stimulated Supercontinuum Generation," Phys. Rev. Lett. **101**, 233902 (2008).
18. T. Godin et al. Advances in Physics : X **7**, 2067487 (2022).
19. P. Robert, C. Fourcade-Dutin, R. Dauliat, R. Jamier, H. Muñoz-Marco, P. Pérez-Millán, H. Maillotte, J. Dudley, P. Roy, D. Bigourd "Spectral correlation of Raman assisted four-wave mixing generated in a photonic crystal fiber pumped by a chirped pump pulse," Optics Letters 45, 4148 (2020).
20. C. Fourcade-Dutin, A. Imperio, R. Dauliat, R. Jamier, H. Muñoz-Marco, P. Pérez-Millán, H. Maillotte, P. Roy and D. Bigourd, "Temporal distribution measurement of the parametric spectral gain in a photonic crystal fiber pumped by a chirped pulse" Photonics **6**, 20 (2019).
21. C. Fourcade-Dutin and D. Bigourd "Near infrared tunable source delivering ultra-short pulses based on an all normal dispersion fiber and a zero dispersion line" Appl. Phys. B 124, 154 (2018).
22. E. Genier, P. Bowen, T. Sylvestre, J. M. Dudley, P. Moselund and O. Bang, "Amplitude noise and coherence degradation of femtosecond supercontinuum generation in all-normal dispersion fibers" J. Opt. Soc. Am. B **36**, A61 (2019).
23. A. M. Heidt, J. S. Feehan, J. H. V. Price and T. Feurer, "Limits of coherent supercontinuum generation in normal dispersion fibers" J. Opt. Soc. Am. B **34**, 764 (2017).
24. K. Inoue and T. Mukai, "Experimental Study on Noise Characteristics of a Gain-Saturated Fiber Optical Parametric Amplifier," J. Lightwave Technol. 20, 969(2002).
25. J. M. Dudley, G. Genty and S. Coen, "Supercontinuum generation in photonic crystal fiber," Rev. Mod. Phys. **78**, 1135 (2006).
26. C. Fourcade-Dutin, F. Fauquet, P. Mounaix, D. Bigourd, "Chirped Pulsed Four-Wave Mixing Spectrogram retrieval from single shot spectrum measurement" *IEEE Phot. Technol. Lett. Submitted.*
27. C. Fourcade-Dutin and D. Bigourd, "Modulation instability in a dispersion oscillating fibre pumped by a broad band pulse," J. Mod. Opt. **64**, 500 (2017).
28. N. Nishizawa and J. Takayanagi, "Octave spanning high-quality superontinuum generation in all-fiber system" J. Opt. Soc. Am. B **24**, 1786 (2007).
29. Y. Liu, Y. Zhao, J. Lyngso, S. You, W.L. Wilson, H. Tu and S.A. Boppart, "Suppressing short-term polarization noise and related spectral decoherence in all-normal dispersion fiber supercontinuum generation" J. Lightwave Technol. **33**, 1814 (2015).